Survival of Molecular Reaction Control in a Bistable System in Condensed Phase

Ignacio R. Solá, Raul Muñoz-Sanz, and Jesus Santamaria*

Departamento Quimica Fisica I, Universidad Complutense de Madrid, E-28040 Madrid, Spain

Received: October 8, 1997; In Final Form: January 6, 1998

In this paper we are concerned with the efficiency and robustness of different optimal pulses that drive the isomerization reaction in a bistable potential. The perturbation is treated as a random-phase strong oscillation that shifts the energy barrier. We show how the reaction can be controlled by means of very intense single Gaussian pulses or linear combinations of these pulses and how the control can survive after the perturbing action. The actual resistance to the bath effects changes with the scheme used, and we concentrate on the different behaviors for different bath frequencies. In particular pump−probe schemes offer stabilizing properties at some frequency windows of the bath spectral range. We also address the problem of phase sensitivity and we find the presence of phase nodes, which are particular values of the bath frequency where the reaction dynamics is almost insensitive to the actual phase of the bath oscillations.

1. Introduction

Optimal control theory (OCT) of molecular systems has by now developed a few general physical schemes[1] whose validity has been experimentally verified in some cases.[2] The great majority of the effort was placed on the isolated molecule case, and some arguments have been prompted against the ability of these phase-sensitive schemes to survive after the strong decoherence mechanisms found in condense matter. Between some recent attempts to treat the bath effects on the "optimal" dynamics, we outline the use of a semiclassical phase-space representation in the perturbation limit by Wilson et al.,[3] the use of a pure-dephasing bath in the Markov approximation by Sugawara and Fujimura,[4] or even beyond some approximations for resonant baths by Korolkov et al.[5] In a very recent work close in spirit to the present contribution, Cao[6] showed both the effectiveness and robustness of a positive chirped pulse in order to assure absorption in the UV.

In this paper we address the question of controlling an isomerization reaction[7,8] and exploring the robustness of the control strategies under different bath perturbations. We concentrate our attention in the case of very low barrier reaction and strong nonresonant perturbation using very simplistic models. The unperturbed system is an asymmetric bistable potential chosen to represent a generic unimolecular process such as an isomerization reaction or a proton transfer. Several IR optimal fields in the femtosecond regime are found that lead the system from the left, deeper well to the right one, representing distinct physical strategies that realize the reaction. In particular we are interested in experimentally feasible fields expressed as single Gaussian-shaped pulses or linear combinations of Gaussian-shaped pulses. In contrast with the schemes developed by the groups of Paramonov and Manz,[7] we concentrate on very short time dynamics, and therefore the excited wave packet is never an eigenstate of the system, but rather a broad coherent superposition of the eigenstates of the system. We study the sensitivity of the reaction yield with respect to the different parameters that shape the fields, and we also address the question of phase sensitivity of the optimal pulses. Then we consider the system immersed into the bulk of a bath very simply modeled by a single frequency of the spectral density and phase-averaged with respect to the laser field. We show how much of the reaction control survives using the different optimal pulses for several values of bath−system coupling and of bath frequency. In particular it is found that certain control scenarios prove to be more robust for specific conditions of the bath (frequency windows in the spectral density), while others seem to be more insensitive in the whole range of the numerical experiment. The degree of phase sensitivity related with the phonon−system coupling is also shown. In a general context, we endeavor to reveal the most suited strategies that control the reactive event for this kind of system, extending the validity of the model to perturbations including a whole spectral distribution of frequencies and implicit decoherent mechanisms.

The outline of the paper is the following. In section 2 we give a brief description of the system and the perturbation to which it is subjected. In section 3 we examine the recipe employed to find the set of optimal fields. Then in section 4 we first analyze the dynamics of the system driven by the optimal fields, trying to unravel the physical mechanisms underlying the reaction. Then we switch on the perturbation and comment on the sensitivity of the schemes to the different parameters that define the coupling of our system with the environment. Finally we conclude in section 5 with the summary and prospects.

2. The System

The system that undergoes the reaction is a bistable potential bearing two localized states in the deeper left well, $|L_0\rangle$ and $|L_1\rangle$, only one localized state in the right well, $|R_0\rangle$, and a set of (infinite) delocalized states $|D_n\rangle$, the first of them being exactly at the top of the barrier, which we differentiate from the others by the distinct label of $|B\rangle$. The potential energy with the energy levels is shown in Figure 1. It is defined by the formula

$$V(x) = D + f_c^0 \frac{\omega_b x}{2} - \left(\frac{\omega_b x}{2}\right)^2 + \frac{1}{4D}\left(\frac{\omega_b x}{2}\right)^4 \qquad (1)$$

* E-mail: jesus@hp720.quim.ucm.es.

S1089-5639(97)03278-7 CCC: $15.00
Published on Web 02/28/1998

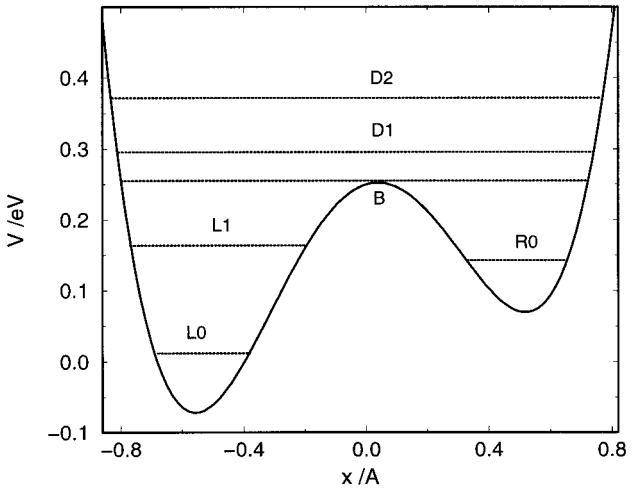

Figure 1. Potential energy and energy levels for the bistable system.

where the quadratic parameters are chosen to represent an intramolecular proton-transfer reaction (in particular the energetics is roughly representing the malonaldehyde proton-transfer reaction).

The values of the parameters are $f_c^0 = 10^{-2}$ amu·Å/fs, $\omega_b = 1392.6$ cm^{-1}, and $D = 0.25$ eV (2089 cm^{-1}). The reduced mass is always taken as 1 amu, and the dipole function is simply the reaction coordinate (centered at the top of the barrier) $\mu = x$. All scaling factors are included in the electric field amplitude. Since the system has no center of symmetry, there are no symmetry rules and all transitions are allowed. The strongest dipole matrix elements couple states L_0 with L_1, L_1 with B and D_1, B with D_1 and R_0, and D_1 with R_0 and D_2.

To include the coupling of the bath with the system, we consider a perturbation of the form

$$V_c = A_c \frac{\omega_b x}{2} \cos(\omega_b t + \phi_s) \tag{2}$$

and we test for different values of the parameters the sensitivity of the system with respect to the amplitude of the perturbation (A_c goes from 10% to 75% of f_c^0) and frequency of the bath (ω_b goes from 20 to 333 cm^{-1}). We point out that these conditions imply a regime of severe perturbation, where the landscape of the potential barrier changes at least 10% of its value at rest. We carry out simulations changing the initial phase of the perturbation in the entire range ($0-2\pi$), and the final results that we show are phase-averaged.

From a time-independent point of view, the net effect of the perturbation will be to blur the energy of the system eigenstates. This energy uncertainty (in the presence of radiation coupling) implies the overlapping of the states $|B\rangle$ and $|D_1\rangle$ but does not change the number of energy levels inside the wells.

3. Method

There are a few methodologies (or recipes) to set up and solve the equations that assure optimal pulse shaping. For a comparison we address the readers attention to ref 9. Here we start assuming the full variational procedure of Rabitz[10] and further impose the shape of the field as a linear combination of Gaussian-shaped pulses:

$$\epsilon(t) = \sum_i A_i \exp\left[-\frac{1}{2}\left(\frac{\tau - \tau_{0,i}}{\Gamma_i}\right)^2\right] \cos(\omega_i t) \tag{3}$$

So we are looking for the set of optimal parameters $\{\omega_i, \Gamma_i, \tau_{0,i}, A_i\}$ such that the probability of finding the system in the right well at time T, $|\langle R_0|\psi(T)\rangle|^2$, is a local maximum (where $\psi(t)$ represents as usual the system wave function).

Say, if ξ_i is any of the parameters that define the field, the variational optimal control procedure implies that at the maximum the optimal parameters obey the following equation:[11]

$$\xi_i = \int_0^T \mathcal{T}\left(\langle\chi(t)\left|\frac{\mu}{\hbar}\right|\psi(t)\rangle\right) \frac{\partial\epsilon(t)}{\partial\xi_i}\,dt \tag{4}$$

where $\mathcal{T}$ stands for the imaginary part. Both $\psi(t)$ and $\chi(t)$ are wave functions that follow the time-dependent Schrödinger equation (TDSE) with initial conditions

$$|\psi(0)\rangle = |L_0\rangle \tag{5}$$

$$|\chi(T)\rangle = |R_0\rangle\langle R_0|\psi(T)\rangle \tag{6}$$

where $\chi(T)$ is actually the Lagrange multiplier in the OCT problem and it carries the information of the part of the system that has reached the physical objective at time T. Formula 4 then links the optimal parameters with the matching of the full wave function and the part of the system that is already moving to the desired target, via the dipole moment μ.

The TDSE equations are solved by using the split−operator algorithm,[12] and the optimal field equation is solved iteratively using a gradient method.[13] We emphasize that no immediate feedback algorithm (as in the Krotov method[9]) can be used when the field is parametrically optimized. The optimal parameters provide the functional form of the field and implicitly depend on it, through the wave function dynamics at all times.

4. Results and Discussion

4.1. Search for the Optimal Pulses. In this section we attempt to find several optimal pulses in order to drive the isomerization reaction from the left well (initial state is $|L_0\rangle$) to the right well (final state is $|R_0\rangle$) of our potential.

The optimal pulse implicit equation has in most cases multiple solutions. First there is a set of outside parameters that easily induce different solutions (and even distanced solutions in the topological space of the pulses) which are related to experimentally controlled parameters, such as the time duration of the pulse T, the number of Gaussian-shaped pulses to be used (like in pump, pump−dump, pump−pump−dump experiments), and the set of free parameters to be optimized (the width of the Gaussian, the carrier frequency, the intensity, etc., or even a set of parameters defining a different functional form for the pulse). Moreover depending on the initial conditions, the iterative process in general leads to different results, and the experienced researcher may use guess pulses of different kind to induce the desired optimal pulse. Finally, we can resort to different methodologies to solve the equation (when we omit the restriction of the functional shape).

Of course there will be one of these optimal pulses to be considered as the "most optimal pulse", but all of them drive the system to local maxima of the transition probability from $|L_0\rangle$ to $|R_0\rangle$. Also, the behavior of the pulse can change dramatically with the occurrence of the perturbation, and therefore we search not only for an optimal efficient pulse but also for a robust one. We defer the discussion of this feature to the next section.

In Table 1 we show the parameters that define the optimal pulses obtained that will serve for further discussions in the

TABLE 1: Parameters that Define the Form of the Optimal Pulses[a]

	200 fs			400 fs				1 ps
	ISP	WLP	PDP	APD	SPD	PLD	LPD	CW
ω_i/cm^{-1}	1209	1192	1200	1226	1192	1209	2047	1093
			1246	1265	1450	1253	970	
Γ_i/fs	40.0	63.3	40.0	37.8	40.3	40.0	128.4	320.0
			70.0	72.4	40.1	120.0	56.1	
$t_{0,i}$/fs	100.0	100.3	60.0	60.0	90.1	90.0	127.9	500.0
			110.0	305.2	309.9	200.0	343.7	
A_i/(10^7 V/cm)	3.92	2.80	2.84	2.76	3.13	2.97	3.63	1.2
			1.26	1.17	2.10	0.57	1.91	

[a] Acronyms are used to define the different optimal pulses. The nomenclature is the following: ISP stands for intense short pulse; WLP stands for weak long pulse; PDP stands for pump−dump pulse; APD stands for asymmetric pump−dump; SPD stands for symmetric pump−dump; PLD stands for pump and longer dump; LPD stands for longer pump and dump; and CW stands for continuous wave field (more than 1 ps).

TABLE 2: Reaction Yields (in Percent) Induced by the Optimal Pulses in the Presence of the Bath, for Different Bath Frequencies ω_b and for Two Values of Bath Coupling, $A_c = 0.1f_c^0$ and $A_c = 0.4f_c^0$ (Above and Below Values in Each Row, Respectively)[a]

	200 fs			400 fs				1 ps
ω_b	ISP	WLP	PDP	APD	SPD	PLD	LPD	CW
0	74.7	72.5	82.5	86.1	75.3	83.6	69.6	41.0
20	69.0	62.2	72.7	34.2	49.0	56.7	27.8	13.0
	30.5	19.5	24.3	13.9	23.5	22.1	13.9	6.9
40	69.1	62.4	73.0	39.7	50.3	60.4	29.6	9.1
	30.4	19.5	25.4	13.9	20.6	23.7	13.9	2.1
80	69.3	63.3	74.2	65.2	59.4	70.2	45.0	15.1
	30.2	17.8	25.5	11.1	19.5	19.7	11.1	5.0
100	69.4	63.8	75.0	76.2	65.9	74.7	52.7	21.0
	30.1	16.9	24.3	7.2	17.2	14.8	7.2	6.6
120	69.6	64.3	76.0	80.9	71.2	78.6	57.5	18.8
	30.1	16.2	23.4	22.2	28.3	15.3	22.2	19.5
150	69.9	65.1	76.8	81.3	73.5	80.3	59.9	5.0
	30.3	15.7	24.2	35.7	33.9	31.0	35.7	15.4
200	70.5	66.4	78.1	82.0	70.8	78.0	60.1	40.3
	31.8	17.2	28.3	19.4	20.3	24.9	19.4	13.9
333	72.2	69.3	78.3	58.6	65.8	73.3	60.5	40.4
	43.6	36.0	35.9	3.5	16.7	18.8	3.5	35.2

[a] The nomenclature is the following: ISP stands for intense short pulse; WLP stands for weak long pulse; PDP stands for pump−dump pulse; APD stands for asymmetric pump−dump; SPD stands for symmetric pump−dump; PLD stands for pump and longer dump; LPD stands for longer pump and dump; and CW stands for continuous wave field (more than 1 ps).

paper, and the key for the nomenclature follows. In the first row of Table 2 we show the results obtained by the optimal fields (reaction yields). Here we will comment on the mechanisms they force into the system to achieve the reactive event, their distinct features, and other solutions explored. In Figure 2 we show the time evolution of the transition probabilities for four typical cases. A word of caution for the nomenclature employed, which can be misleading: the terms used serve only for internal comparison between the different cases, and therefore even a weak and long pulse should be understood in a context of very strong fields in the femtosecond regime (intensities above 10^{10} W/cm^2). In particular, CW makes reference to fields whose Gaussian width (fwhm) is greater than 1 ps.

We start with the case of single Gaussian-shaped pulses. For short times ($T = 200$ fs) we have the prototype cases of ISP (intense short pulse) and WLP (weak long pulse). In both cases the dynamics show a two-step mechanism, first with absorption of energy above the barrier and then with emission. In the first step, an average absorption of two to three photons drives the system to transient nonresonant populations (at very short times we don't have energy resolution yet) in the sequence $|L_0\rangle \rightarrow |L_1\rangle \rightarrow |B\rangle \rightarrow |D\rangle \rightarrow |B\rangle \rightarrow |D\rangle$. After populating the delocalized states, one or two photons are emitted, finally reaching the desired $|R_0\rangle$ state on the other well. So, one single pulse is enough to saturate the upper levels and stimulate emission, with the transient populations allowing the induced dipole for the next photons to project essentially on the right well. When the intensity of the field increases (ISP), the number of photons absorbed (and at the end, emitted) is higher, and several states above the barrier are reached; the beating is produced between odd and even (including the barrier state) delocalized states. This is shown in Figure 2A. By changing the intensity of the pulse, we essentially can choose the final excited state selected, $|D_1\rangle$ or $|R_0\rangle$. If we seek less intense pulses, in order to assure equally proficient yields, we have to increase the width of the pulse, as in the WLP case. Also the carrier frequency is slightly shifted from the energy difference between the first two levels in order to facilitate the two-photon absorption from $|L_0\rangle$ to $|D_1\rangle$. Nevertheless the results are less sensible to both these parameters than to the intensity. The other parameters take a minor role; for instance, the phase of the pulse is almost unimportant, inducing changes in the result of less than 2%.

When exploring optimal pulses at even shorter times (100 fs), the same general behaviors were obtained, but with lower yields, since the final step of emitting energy competed with the parasite process of absorption, and we had in general a linear absorption of energy until the field was switched off. For very high intensities, the maximum of the probability in the $|R_0\rangle$ state was achieved at shorter times, in less than 50 fs.

We also tested the proficiency of CW fields with frequency matching the direct transition from the initial to the final desired

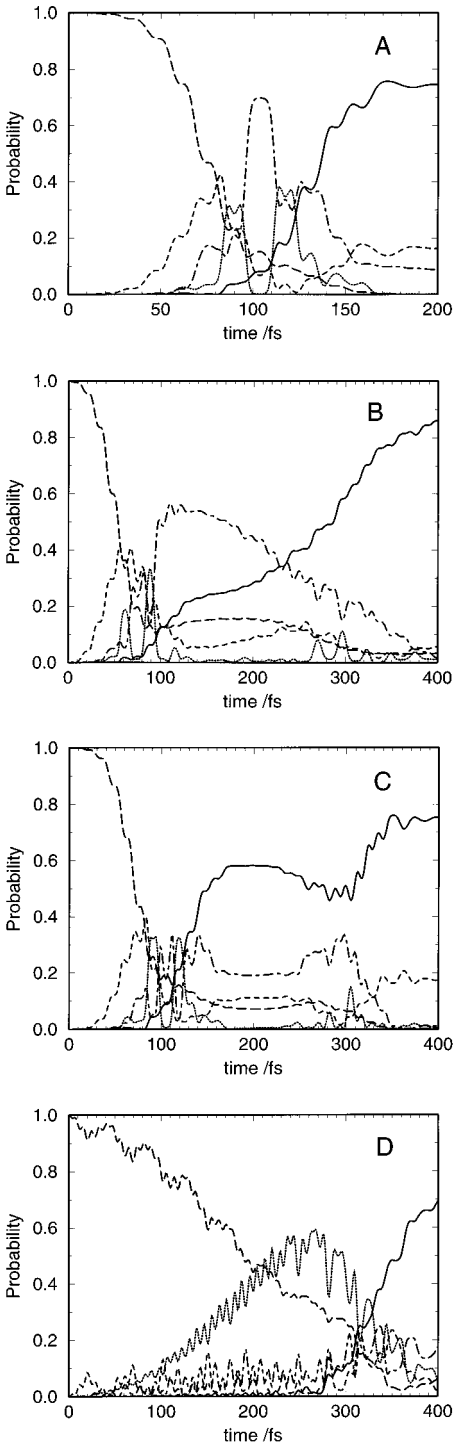

Figure 2. Time evolution of the system driven by the optimal pulses: (A) ISP (intense short pulse); (B) APD (asymmetric pump−dump); (C) SPD (symmetric pump−dump); (D) LPD (longer pump + dump) followed through transition probabilities to the energy levels. The populations of the different levels are represented by the following lines: long-dashed line for $|L_0\rangle$; solid line for $|R_0\rangle$; dashed line for $|L_1\rangle$; dotted line for $|B\rangle$; and dot−dashed line for $|D_n\rangle$.

state. Yet for 1 ps, this tunnel-induced reaction does not provide yields comparable with those obtained by the aforementioned pulses.

In the next step we tested a linear combination of two Gaussian-shaped pulses. For $T = 200$ fs the optimal pulse obtained, PDP (pump−dump pulse), looks like a single Gaussian function with a long tail at the end. The physical realization of the optimal dynamics seems similar to that of the single Gaussian pulses, but now the pump pulse is a weaker version of the ISP, and the decrease in the amplitude is enough to populate selectively the $|D_1\rangle$ state, while the dump pulse puts into resonance states $|D_1\rangle$ and $|R_0\rangle$ and enables faster emission of photons. Nevertheless both pulses overlap in time, and the emission process begins while the states above the barrier are still interchanging. The pump−dump scheme allows a rise in the yield of more than 10% with respect to single Gaussian schemes. For $T = 400$ fs more possibilities are offered. In the APD (asymmetric pump−dump) case, we simply increase the time delay between the pump and the dump pulses. Now this delay avoids any parasite process in the emission procedure. We show the time evolution of the transition probabilities in Figure 2B. In the SPD (symmetric pump−dump) case, the first pulse amplitude is midway between the weak and the strong cases, inducing mainly the selection of the $|R_0\rangle$ state, but also in equilibrium with the excited population in $|D_1\rangle$ and $|L_1\rangle$, which are afterward deployed by the dump pulse. In this case, as can be seen in Figure 2C, the pump pulse shifts the population from $|L_0\rangle$ to $|R_0\rangle$ (with upper states as intermediates), and it alone is responsible for a yield of 0.583. The dump pulse plays a minor role, increasing the yield to 0.753 (30% improvement).

We also tested schemes where a longer resonant field was used either as a pump or as a dump pulse. In the PLD (pump + longer dump pulse) case we use a pump pulse very similar to that used in SPD and a longer time field, which is switched on all the time, and according to its carrier frequency should allow first the absorption from $|L_0\rangle$ to $|L_1\rangle$ and finally the emission from $|D_1\rangle$ to $|R_0\rangle$. The dynamical behavior and results obtained resemble closely that of the SPD case, the essential difference being that now we use as a dump a much weaker field (the longer field intensity is at least 1 order of magnitude lower than that of the Gaussian-shaped pulses). In the LPD (longer pump + dump pulse) case, we first use a longer time field to pump population from the initial state to the barrier state $|B\rangle$, and then we deploy this state using a Gaussian-shaped dump pulse. The dynamical behavior in this case is much simpler, since many of the transient and strong field effects are not present now. We show this behavior in Figure 2D.

From a general point of view, for two Gaussian-shaped pulses the space of parameters duplicates its dimensionality and one may expect an increase in the number of solutions (we show some different types as samples, which of course do not cover all possibilities). But the sensitivity of the different parameters is almost the same, except for the relative phase between the pulses. For this parameter the pump−dump scheme shows great sensitivity, and the particular choice may induce no dump of energy at all! When we use longer time fields as pump or dump pulses, the degree of sensitivity decreases. For example, we observe a variation of the yield from 0.86 to 0.10 in the APD case and from 0.70 to 0.43 in the LPD case.

4.2. Perturbation Effects on the Optimal Dynamics. In Table 2 we show a résumé of the yields of reaction obtained after "immersing" the system into the bath, using the same optimal pulses, for different values of the bath frequency (in rows) and for two values of the amplitude of the oscillation, $A_c = 0.10f_c^0$ and $A_c = 0.40f_c^0$ (above and below values in each row, respectively). We also have results for $A_c = 0.25f_c^0$ and $A_c = 0.75f_c^0$ that are not shown in the table. Each yield represents an average over the entire range of values of the initial phase of the perturbation.

We first read the table from left to right, in order to make a rough comparison of the resistance of the pulses to the bath action. By following in detail the dynamics of the driven

perturbed system, we have noticed that the perturbation interferes more strongly with the emission process than with the absorption. All phase-dependent schemes (pump−dump for instance) are more likely to be disturbed by the bath, which can change completely the actual behavior of the dump pulse. Also the perturbation is more efficient at longer times, and very intense pulses leading to high-energy absorption are less affected by the minor oscillation of the bath, which mainly changes the landscape of the potential around the wells and barrier.

With only these general remarks we can already compare on the average the robustness of the different optimal pulses. First, single Gaussian pulses should be more robust than two Gaussian pulses (at least when the dump pulse is mainly responsible for the final yield and the scheme is highly phase sensitive). Second, short time schemes are preferable to long time schemes (so the Gaussian width here is the key parameter). Third, very intense pulses leading to high-energy absorption are more robust than weaker ones. Finally the most sensitive schemes will be those implying resonant routes and tunneling reaction, since the perturbation will degrade the quality of the frequency matching and will inhibit the tunneling rate. With these trends at hand we can understand the "hierarchy of stability" of the pulses versus the intensity of the perturbation, which goes from ISP to SPD, PDP, WLP, PLD, APD, and finally LPD (or CW) in descending order of stability (here we consider stability the ratio between the perturbed yield and the optimal yield in the absence of bath). Schemes like SPD occupy a very high place in this "ranking" because the pump pulse is already responsible for leading the reaction (and by means of a short pulse), while the role of the dump pulse is reduced to deploy what remains in the excited levels.

Now we read the table by columns in order to extract detailed information about the dependence of the dynamics with the bath frequency. In Figure 3A we show this dependence for three optimal pulses and for a comparatively low value of the time-dependent perturbation amplitude A_c. In the ISP case we see a very slow increase in the yield (greater stability) for higher bath frequencies. For higher values of A_c or for the WLP and PDP cases, the same behavior is seen, although now the effect of stabilization at high frequencies is stronger. The behavior is completely different for the SPD, PLD, or APD pulses. In these cases the efficiency of the pulse shows oscillations with maximum values for middle or high bath frequencies. This effect is clearer for the APD pulse, and in Figure 3B we show for this case how as A_c is increased, there appear sharper windows in the bath spectral range where the pulse efficiency is greater. The same phenomenon has been observed for the SPD and the PLD pulses. Taking these facts into account, we can choose different optimal pulses depending on the spectral distribution of the bath, whether it is centered at low, middle, or high values of frequencies. For very high values of A_c the perturbation almost destroys the efficiency of the pulses and the behavior with respect to bath frequency is less clear (in a sense the windows where the efficiency is greater converge into a fast oscillating dependence).

Finally we are concerned with the sensitivity of these optimal dynamics with respect to the phase of the bath-induced oscillations. The other parameters of the bath coupling, ω_b and A_c, can be more or less controlled by choosing a particular bath or temperature. But the initial phase of the perturbation, ϕ_b, is both uncontrolled and unknown. Moreover if we concentrate on the liquid in bulk, there are incoherent mechanisms that would imply the changing of phase during the time evolution of the system. Therefore we would like to have optimal pulses leading to reactions as independent of ϕ_b as possible. In general terms we observe lower sensitivity for low values of A_c and from very low ω_b to very high ω_b. To give a rough measure of the variation of the results induced by the perturbation phase, we have averaged the yields obtained for all phase and frequency values and we measured the dispersion of these results. Since the variation induced by phase is much faster than that induced by frequency, the statistics should reflect mainly the dispersion of the values caused by ϕ_b. We show this in Table 3. The table data reflect the greater dispersion at increasing A_c (but for higher values the overall effect of control suppression makes the dispersion also decrease) and give a picture of the robustness of the pulses close to the "ranking" we had already inferred from the averaged values.

What is left from the statistics seems more interesting. For

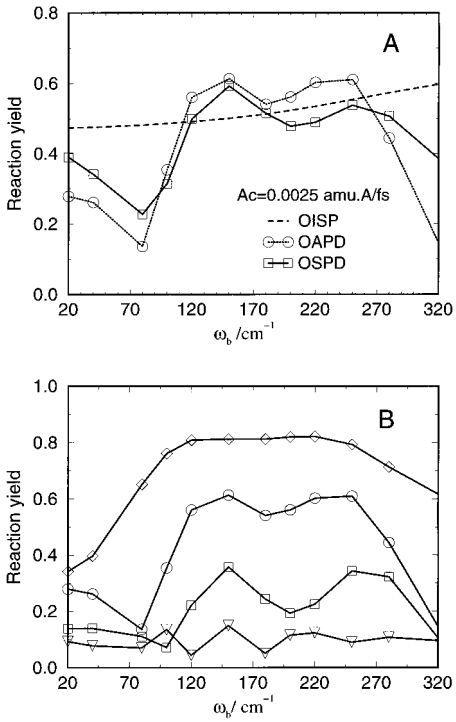

Figure 3. Effect of bath frequency (ω_b) and bath coupling intensity (A_c) in the reaction driven by the optimal fields. In A we show the reaction yields for three different pulses, ISP (intense short pulse), APD (asymmetric pump dump), and SPD (symmetric pump dump) with $A_c = 0.25f_c^0$ fixed. In B we show the reaction yields for the APD case and for different values of the coupling. From top to bottom, $A_c = 0.10$, 0.25, 0.40, and $0.75f_c^0$.

TABLE 3: Dependence of the System on the Perturbation Phase[a]

	$A_c = 0.1f_c^0$	$A_c = 0.25f_c^0$	$A_c = 0.4f_c^0$
ISP	70 ± 6	50 ± 13	33 ± 15
WLP	65 ± 11	40 ± 17	20 ± 25
PDP	76 ± 5	51 ± 17	28 ± 16
APD	69 ± 20	42 ± 23	20 ± 16
SPD	70 ± 13	44 ± 15	24 ± 16
PLD	74 ± 10	46 ± 16	24 ± 15
LPD	52 ± 17	21 ± 13	6 ± 5

[a] We give the average and dispersion values of the yield (both in percent) for all bath frequencies and phases. The nomenclature is the following: ISP stands for intense short pulse; WLP stands for weak long pulse; PDP stands for pump−dump pulse; APD stands for asymmetric pump−dump; SPD stands for symmetric pump−dump; PLD stands for pump and longer dump; LPD stands for longer pump and dump; and CW stands for continuous wave field (more than 1 ps).

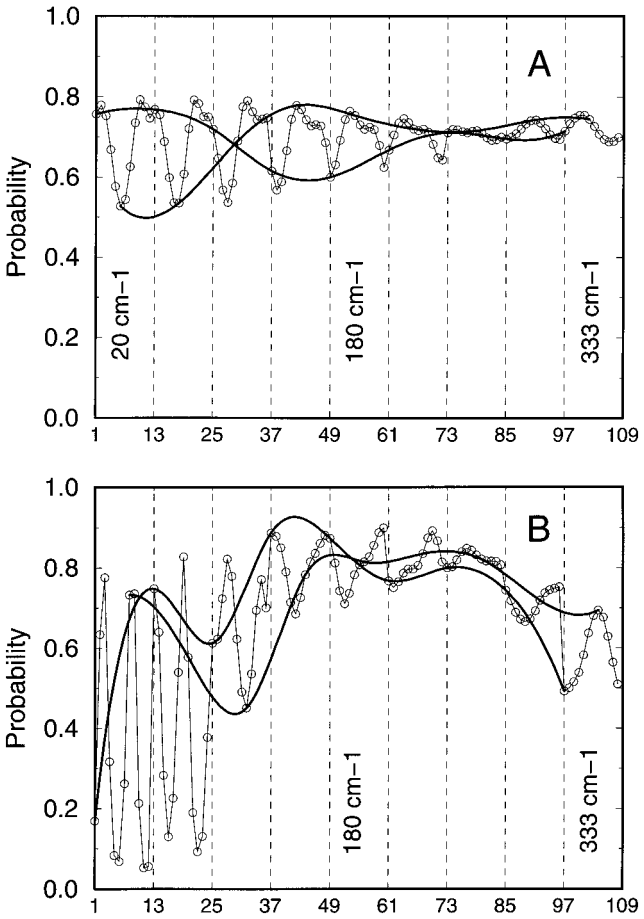

Figure 4. Bath-phase dependence of the reaction yields for the ISP case (intense short pulse) in A and for the APD case (asymmetric pump−dump) in B. $A_c = 0.1f_c^0$ is fixed for both cases. Between vertical lines we display the results for ϕ_b ranging from 0 to 2π, and from left to right the overall variation with increasing ω_b. We superimpose the lines that join values for the same phase at different frequencies.

certain values of bath frequency we have seen that the yields were almost fully phase independent. We refer to nodes to these particular values of ω_b. For the cases of ISP, WLP, and PDP (those that show greater efficiency for higher ω_b) the nodes appear for middle or high values of the frequency. Most intriguing, for the APD, SPD, and PLD cases, the nodes show up at the spectral windows. In Figure 4 we show the variation of the yields with phase ϕ_b and frequency ω_b for the optimal pulses ISP and APD and fixed value of A_c ($A_c = 0.001$ uma·Å/fs). Between vertical lines we display the results for ϕ_b ranging from 0 to 2π, and from left to right the overall variation with increasing ω_b. Also shown are lines that link the different results for a fixed value of the phase (0 or π) as ω_b increases. For the ISP case, we see one "node" around 200 cm^{-1}, although in general the whole dynamic behavior is quite independent of the phase and frequency of the bath. For the APD case at low frequencies the proficiency of the pulse will highly depend on the relative phase of the bath, but for ω_b also around 200 cm^{-1} we have both higher values of the yield and phase insensitivity.

5. Summary and Conclusions

In the present paper we have explored different physical schemes that drive the isomerization reaction of a simple system by means of femtosecond IR pulses. The goal was to test the efficiency and robustness of the schemes in the presence of environment perturbations. The chosen system was a bistable potential with only three localized states between both wells, and the bath was modeled by a monochromatic wave modulating the amplitude of the barrier. We tested the resistance of the reaction control for different values of the frequency and amplitude of the perturbation. The relative phase of the bath field with respect to the system was kept fixed during the laser action, but the initial conditions were sampled and averaged. The chosen pulses were obtained by optimizing the parameters that define Gaussian-shaped pulses or linear combinations of the former, using a gradient method algorithm in the frame of OCT.

With respect to the efficiency of the pulses we have compared single Gaussian versus double Gaussian schemes, and intense short pulses versus weak long pulses (which in the limit of our time selection we called CW fields). From this outset we have seen that the most sensitive parameters are the intensity of the pulse, the fwhm, and the carrier frequency in the given order. For very short time experiments (100 fs) only very intense pulses could provide reaction yields over 50%. Increasing the pulse duration, weaker pulses with improved yields could be obtained. In all cases the dynamic evolution of the system implied absorption of energy above the barrier and the successive emission of photons projecting from the system into the left well. Qualitatively the dynamics was mainly governed by transient effects and strong laser field phenomena. Of course, single Gaussian schemes can provide acceptable yields in isomerization reactions only where the barrier is very shallow as in the present study. We have seen that double Gaussian schemes simulating pump−probe experiments always improved the reaction yields, by refining the basic mechanism of fast absorption followed by emission of photons, but with the drawback of important phase sensitivity. The realization of this pump−probe scheme was only clear for greater time scales (400 fs) where the pulses did not overlap. In this scenario we have seen that longer time fields could be used either as a pump or dump pulse, allowing a decrease in the intensity of the field and reducing the degree of phase sensitivity. Resonantly enhanced mechanisms become more important, but only for time scales above picosecond can the tunneling rates to reaction compete with the multiphoton routes.

With respect to the robustness of the previous pulses we have compared the resistance of the optimal dynamics with the effect of increasingly strong perturbations with different frequencies (ω_b). We have seen that the perturbation mainly interferes with the emission process of the dynamics, and its action is more efficient at longer times and at low energies. Resonant-based mechanisms and phase-sensitive schemes are the least robust strategies, while the very fast and intense processes, though not very efficient, are the most robust. To minimize the effects of the strong perturbation, the fields should be stronger than the oscillatory perturbation during all the processes of absorption, crossing the barrier, and emission, as shown by Korolkov et al.[5] The balance between the optimal efficiency and the resistance to perturbation at different bath frequencies makes the choice of the "most optimal pulse" not unique, but changing with the environment conditions. For instance, we have seen that the short time pulses (ISP, WLP, and PDP) show greater resistance to the perturbation at higher bath frequencies, while longer time pulses (APD, SPD) show greater efficiency at certain values of the bath spectral range, which we called frequency windows. On the other hand, the phase dependence with the bath is usually lower at smaller bath couplings and higher bath frequencies, and for certain values of ω_b there was almost no phase dependence at all. We called phase nodes the spectral

range with these phase stabilization properties, and most intriguing we have observed that these nodes appeared at the aforementioned frequency windows for the pump−dump optimal pulses. Therefore short intense pulses are the choice at higher ω_b, but for certain intervals the pump−probe schemes seem more fruitful. Also, the coincident properties of frequency windows (or essentially frequency independence in a whole range) and phase nodes make plausible that these conclusions can be extended to more complete descriptions of the bath, including implicit decoherent mechanisms and a wider spectral (not monochromatic) range as the bulk of a liquid. Therefore we think that we can be confident about the survival of control mechanisms in realistic condensed phases even at the strong perturbation conditions explored in this paper.

References and Notes

(1) We give here only the references to recent review articles where the interested reader can search for a complete bibliographical account: Brumer, P.; Shapiro, M. *Annu. Rev. Phys. Chem.* **1992**, *43*, 257. Tannor, D. J. in *Molecules in Laser Fields*; Bandrauk, A., Ed.; Dekker: New York, 1994. Neuhauser, D.; Rabitz, H. *Acc. Chem. Res.* **1993**, *26*, 1581.

(2) Shnitman, A.; Sofer, I.; Golub, I.; Yogev, A.; Shapiro, M.; Chen, Z.; Brumer, P. *Phys. Rev. Lett.* **1996**, *76*, 2886. Bardeen, C.; et al. To appear in *Chem. Phys. Lett*.

(3) Krause, J. L.; Whitnell, R. M.; Wilson, K. R.; Yan, Y. J. In *Femtosecond Chemistry*; Manz, J., Woeste, L., Eds.; VCH: Weinheim, 1995. Cao, J.; Messina, M.; Wilson, K. R. *J. Chem. Phys.* **1997**, *106*, 5239.

(4) Sugawara, M.; Fujimura,Y. *J. Chem. Phys.* **1994**, *101*, 6586.

(5) Korolkov, M. V.; Manz, J.; Paramonov, G. K. *J. Chem. Phys.* **1996**, *105*, 10874.

(6) Cao, J.; Bardeen, C.; Wilson, K. R. To appear in *Phys. Rev. Lett*.

(7) Combariza, J. E.; Just, B.; Manz, J.; Paramonov, G. K. *J. Phys. Chem.* **1991**, *95*, 10351. Combariza, J. E.; Goertler, S.; Just, B.; Manz, J. *Chem. Phys. Lett.* **1992**, *195*, 393.

(8) Chelkowski, S.; Bandrauk, A. D. *Chem. Phys. Lett.* **1995**, *233*, 185. Jakubetz, W.; Lan, B. L. *Chem. Phys.* **1997**, *217*, 375.

(9) Somloi, J.; Kazakov, V. A.; Tannor, D. J. *Chem. Phys.* **1993**, *172*, 85. Tannor, D. J.; Kazakov, V. A.; Orlov, V. In *Time Dependent Quantum Molecular Mechanics*; Broeckhove, J., Lathouwers, L., Eds.; Plenum Press: NewYork, 1992.

(10) Shi, S.; Rabitz, H. *J. Chem. Phys.* **1990**, *92*, 364.

(11) Shi, S.; Rabitz, H. *J. Chem. Phys.* **1990**, *92*, 2927.

(12) Feit, M. D.; Fleck, J. A., Jr.; Steiger, A. *J. Comput. Phys.* **1982**, *47*, 412.

(13) Press, W. H.; Flannery, B. P.; Teukolsky, S. A.; Vetterling, W. T. *Numerical Recipes*, 1st ed.; Cambridge University Press: New York, 1986; Chapter 10.